Published in final edited form as:
Circulation. 2013 July 9; 128(2): . doi:10.1161/CIRCULATIONAHA.112.000768.

The Timing of Myocardial *Trpm7* Deletion during Cardiogenesis Variably Disrupts Adult Ventricular Function, Conduction and Repolarization

Rajan Sah, MD, PhD[1,2], **Pietro Mesirca, PhD**[3,4,5], **Xenos Mason, BSc**[1], **William Gibson, BSc**[6], **Christopher Bates-Withers, BSc**[1], **Marjolein Van den Boogert, BSc**[1,7], **Dipayan Chaudhuri, MD, PhD**[1], **William Pu, MD**[8], **Matteo E. Mangoni, PhD**[3,4,5], and **David E. Clapham, MD, PhD**[1,9]

[1]Howard Hughes Medical Institute, Department of Cardiology, Manton Center for Orphan Disease, Children's Hospital Boston, Boston, MA

[2]Cardiovascular Division, Brigham and Women's Hospital, Boston, MA

[3]CNRS UMR-5203, Institut de Génomique Fonctionnelle, Département de Physiologie, LabEx ICST, Montpellier, France

[4]INSERM U661, Montpellier, France

[5]Universités de Montpellier 1 & 2, Montpellier, France

[6]The Harvard-MIT Division of Health Sciences and Technology, and the MD/PhD Program, Harvard Medical School

[8]Department of Cardiology, Children's Hospital Boston, Boston, MA

[9]Department of Neurobiology, Harvard Medical School, Boston, MA

Abstract

Background—*T*ransient *R*eceptor *P*otential (*TRP*) channels are a superfamily of broadly expressed ion channels with diverse physiological roles. *TRPC1, 3* and *6* are believed to contribute to cardiac hypertrophy in mouse models. Human mutations in *TRPM4* have been linked to progressive familial heart block. *TRPM7* is a divalent-permeant channel and kinase of unknown function, recently implicated in the pathogenesis of atrial fibrillation, however its function in ventricular myocardium remains unexplored.

Methods and Results—We generated multiple cardiac-targeted knock-out mice to test the hypothesis that *TRPM7* is required for normal ventricular function. Early cardiac *Trpm7*-deletion (<E9, *TnT*/*Isl1*-*C*re) results in congestive heart failure and death by E11.5 due to hypo-proliferation of the compact myocardium. Remarkably, *Trpm7*-deletion late in cardiogenesis (~E13, *αMHC*-*Cre*) produces viable mice with normal adult ventricular size, function and myocardial transcriptional profile. *TRPM7* deletion at an intermediate time-point results in 50% of

Correspondence: David E. Clapham, MD, PhD Howard Hughes Medical Institute, Department of Cardiology, Manton Center for Orphan Disease, Children's Hospital Boston, 320 Longwood Ave., Enders 1309, Boston, MA 02115 Phone: 617-919-2680 Fax: 617-731-0787 dclapham@enders.tch.harvard.edu.
[7]Present address: Academic Medical Center, University of Amsterdam, Amsterdam, The Netherlands

Conflict of Interest Disclosures: None.

mice developing cardiomyopathy associated with heart block, impaired repolarization and ventricular arrhythmias. Microarray analysis reveals elevations in transcripts of hypertrophy/remodeling genes and reductions in genes important for suppressing hypertrophy (*Hdac9)* and for ventricular repolarization (*Kcnd2*) and conduction (*Hcn4*). These transcriptional changes are accompanied by action potential prolongation and reductions in transient outward current ($I_{to;}$ *Kcnd2*). Similarly, the pacemaker current (I_f; *Hcn4*), is suppressed in atrioventricular nodal cells, accounting for the observed heart block.

Conclusions—*TRPM7* is dispensable in adult ventricular myocardium under basal conditions, but is critical for myocardial proliferation during early cardiogenesis. Loss of *TRPM7* at an intermediate developmental time-point alters the myocardial transcriptional profile in adulthood, impairing ventricular function, conduction and repolarization.

Keywords

ion channel; electrophysiology; heart block; cardiomyocyte hypertrophy; potassium channels

INTRODUCTION

Transient receptor potential (TRP) channels are a loosely related family of ion channels that share the properties of cation permeability and minimal voltage sensitivity. With respect to cardiac physiology and disease, most interest to date has focused on the TRPC channels (1/3/4/6), which by permeating calcium can activate calcineurin-NFAT mediated cardiac hypertrophy[1, 2]. TRPC7 and TRPM2, as well, are proposed to mediate myocardial apoptosis[3] and oxidative stress-induced cardiomyocyte death, respectively. Human mutations in TRPM4 have been linked to progressive familial heart block type I (PFHBI)[4] and isolated cardiac conduction block[5], due to impaired TRPM4 SUMOylation and enhanced membrane trafficking. Some forms of triggered cardiac arrhythmia are also postulated to arise from gain-of-function mutations in TRPM4[6]. Interestingly, deletion of TRPM4 in mice exhibits sustained hypertension secondary to enhanced catecholamine release from enterochromaffin cells[7], but is not associated with changes in murine cardiac function or electrical activity.

TRPM7, and its close homolog TRPM6, are unique in that they are ion channels containing a carboxyl terminal kinase. TRPM7 is divalent-permeant (*e.g.*, Zn^{2+}, Mg^{2+}, Ca^{2+}), inhibited by cytoplasmic Mg^{2+} [8], and proposed to be important for magnesium homeostasis[9] (but see refs [10], [11]). Although TRPM7 is ubiquitously expressed, in comparison to other TRPs, it is especially abundant in both human and murine heart[12, 13], and is concentrated in myocardium during embryonic development[10]. Recently, TRPM7 was shown to be up-regulated in atrial fibroblasts harvested from patients with atrial fibrillation (AF). These authors hypothesized that it provided a calcium influx pathway that induced TGF-β1 mediated fibroblast proliferation and differentiation, thereby contributing to atrial fibrosis in the pathogenesis of AF[14]. In neurons, TRPM7 was also proposed to mediate calcium influx contributing to neuronal death in ischemic stroke[15]. Cardiac ventricular fibroblasts have a large TRPM7 current[16] and a TRPM6/7-like current has been recorded from pig and guinea-pig cardiomyocytes[17]. Thus, TRPM7 represents a fascinating, relatively unexplored signaling molecule in cardiac biology that may participate in calcium and/or magnesium signaling via the channel domain and possibly activate downstream signaling pathways via the kinase domain under native conditions or in disease states.

In this study, we show that *TRPM7* is a functional current in freshly dissociated adult murine ventricular cardiomyocytes. The physiological consequences of cardiac-targeted *TRPM7* deletion depend on the timing of *TRPM7* disruption during cardiogenesis. Early *TRPM7*

deletion (*Trpm7 TnT/fl*) induces congestive heart failure *in utero* and embryonic lethality by embryonic day 11.5 (E11.5). By contrast, *TRPM7* deletion in late cardiogenesis (*Trpm7* $^{\alpha MHC/fl}$) has no impact on adult ventricular function, conduction, repolarization, or on the myocardial transcriptional profile. *TRPM7* deletion at an intermediate time-point (*Trpm7* $^{\alpha MHC/-}$) disrupts atrioventricular conduction, ventricular repolarization and ventricular function in adulthood, predisposing to both spontaneous and induced ventricular arrhythmias. Transcriptional analysis reveals reduced expression of several ion channel genes including *Kcnd2*, encoding the important repolarizing transient outward current (I_{to}) in ventricular cells, and *Hcn4*, which encodes the pacemaker current ('funny current'; I_f) in the atrioventricular node (AVN) and conduction system. Consistent with these findings, both I_f and I_{to} are significantly reduced in *Trpm7* $^{\alpha MHC/-}$ AVN and ventricular myocytes, respectively. Taken together, these findings suggest that *TRPM7* is required for a critical period in embryonic cardiac development. The timing of perturbations in *TRPM7* function during cardiogenesis variably affects cardiac function, ranging from arrested cardiac development *in utero*, to longstanding changes in the myocardial transcriptional profile into adulthood, impairing adult ventricular function, repolarization and atrioventricular conduction.

METHODS

See online Supplement for full methods

Cardiac-targeted *Trpm7* knock out mice

All animal procedures have been reviewed and approved by the Institutional Animal Care and Use Committee at Children's Hospital Boston. Cardiac-targeted knockout mice were generated by crossing *Trpm7*$^{fl/fl}$ and *Trpm7*$^{-/fl}$ mice described previously[10] with *TnT-Cre*, *Isl1-Cre* mouse lines (provided by Dr. W. Pu) and *αMHC-Cre* (provided by Dr. M. Schneider). For simplicity, *Trpm7*$^{fl/fl}$ × (*TnT-Cre*) is denoted as ***Trpm7***$^{\mathbf{TnT/fl}}$, *Trpm7*$^{+/fl}$ × (*TnT-Cre*) as ***Trpm7***$^{\mathbf{TnT/+}}$, *Trpm7*$^{fl/fl}$ × (*Isl1-Cre*) as ***Trpm7***$^{\mathbf{Isl1/fl}}$, *Trpm7*$^{fl/fl}$ × (*αMHC-Cre)* as ***Trpm7*** $^{\boldsymbol{\alpha}\mathbf{MHC/fl}}$, and *Trpm7*$^{-/fl}$ × (*αMHC-Cre)* as ***Trpm7*** $^{\boldsymbol{\alpha}\mathbf{MHC/-}}$. Mice were maintained on 129/SvEvTac genetic background.

Embryology

Embryo gestational age was determined from timed matings, with noon of the day of the vaginal plug defined as day 0.5. Embryos were removed from pregnant females euthanized by cervical dislocation between E9-12. For bromodeoxyuridine (BrdU) labeling, pregnant mice were injected intraperitoneally with BrdU (100 μg/g body weight) 1 h before sacrifice and embryo extraction/fixation.

Echocardiography

Echocardiography was performed on conscious mice using a Vevo 2100 ultrasound machine equipped with either a 30 MHz or 40 MHz ultrasound probe (Visual Sonics).

Immunostaining ventricular myocytes and frozen embryonic sections

Freshly dissociated ventricular myocytes and embryonic sections were immunostained using rabbit anti-Troponin-I polyclonal antibody (Santa Cruz, 1:1000 of 200 μg/ml). For BrdU immunostaining of embryonic sections we used rat anti-Brdu monoclonal antibody (Abcam 1:1000 of 1 mg/ml).

Electrocardiography (ECG)

ECGs were performed in supine mice sedated using Avertin anesthesia. Dissection pins were placed subcutaneously in the right arm and left leg. The ECG signal was amplified and then digitized using a Digidata 1320 board (Molecular Devices) acquired with Clampex (pClamp9, Molecular Devices).

Cellular Electrophysiology

TRPM7 current was measured in isolated cardiomyocytes in the whole-cell configuration The voltage protocol (shown in figure insets) held the myocytes at 0 mV, stepped to +100 mV for 40 ms and then ramped down to −80 mV over 500 ms, holding at −80 mV for 40 ms before stepping back up to 0 mV. This protocol was repeated every 4-6 s and recordings continued for 10-15 min per cell until a steady-state TRPM7 current was obtained. Action potentials and potassium currents were measured as previously described[44].

Microarray Analysis

Microarray analysis was performed using Affymetrix Mouse 1.0ST arrays at the Microarray Core Facility at Children's Hospital Boston. Four arrays were used for each group, *WT* (*Trpm7*$^{fl/fl}$*:* 4 hearts and *Trpm7* $^{\alpha MHC/+}$: 4 hearts), *Trpm7* $^{\alpha MHC/fl}$ (8 hearts) and *Trpm7* $^{\alpha MHC/-}$ (8 hearts), and total RNA from 2 hearts were pooled for each array to reduce inter-mouse variability.

qRT-PCR expression analysis

Microarray results were validated by qRT-PCR using the same pooled RNA samples used for microarray analysis (n = 4) from *WT* and *Trpm7* $^{\alpha MHC/-}$ +*HB* groups. For *Trpm7* $^{\alpha MHC/-}$ −*HB* qRT-PCR, RNA from one heart was used per run (n = 4) and compared to the same *WT* group. Real-time PCR reactions were run in triplicate using the SYBR Green method (ROX as passive reference dye; Affymetrix) as previously described[10].

Statistics

All data are represented as means ± S.E.M, unless otherwise specified. All p-values were calculated using the non-parametric Mann-Whitney test when comparing two groups. For multiple comparisons among multiple groups, as in Figure 3 and Supplemental Figure 3, we used the non-parametric version of the ANOVA or Kruskal-Wallis (K-W) test. If the p value from the K-W test was lower than 0.05 we performed Dunn's multiple comparisons test. A p-values less than 0.05 were considered statistically significant.

RESULTS

TRPM7 current in adult mouse ventricular myocytes

We previously showed that TRPM7 is predominantly expressed in the heart of E9.5 embryos[10], and then becomes ubiquitously expressed in later embryonic development[10] and into adulthood[12, 13] . TRPM6/7–like currents have been recorded in pig, guinea pig and rat ventricular cardiomyocytes [17] but the molecular identity of this current was not determined. To confirm that this current arises from *Trpm7*, we first recorded TRPM7-like current from isolated murine adult ventricular cardiomyocytes by applying ramps from +100 to −80 mV over 500 ms from a holding potential of 0 mV. TRPM7-like current on "break-in" is initially absent, but then runs-up over the course of 10-15 minutes to a maximum amplitude at steady state (Figure 1A). The initial currents measured immediately after patch rupture were largely background currents, as these were not inhibited by 10 mM $MgCl_2$ (TRPM7 is inhibited by internal Mg^{2+}; K_D~0.1-0.6 mM[18]). To eliminate the contribution of these background currents from the TRPM7-like current, either Mg^{2+}-inhibited, or "break-in" traces were

subtracted from net current (Figure 1B), revealing the outwardly rectifying current-voltage relationship characteristic of TRPM7.

The gradual run-up of TRPM7 after patch rupture is a feature attributed to either gradual chelation of internal inhibitory Mg^{2+} [18] or dialysis-mediated removal of a diffusible inhibitor. To test whether Mg^{2+} chelation alone would be sufficient to activate TRPM7 in the absence of patch rupture, cardiomyocytes were incubated in 30 μM ethylenediaminetetraacetic acid-aminoester (EDTA-AM), a membrane-permeant form of the divalent cation chelator, EDTA, for 30 min prior to patch-clamp studies. Under these conditions, EDTA-AM treated myocytes yield large outwardly rectifying currents immediately upon break-in (no 'run-up' period required) and these currents are fully inhibited by 10 mM $MgCl_2$ (Figure 1C, D) leaving only the background currents typically seen on break-in under standard whole-cell patch-clamp conditions (Figure 1A). These results suggest that dialysis and chelation of intracellular Mg^{2+} alone is sufficient to activate TRPM7 under whole-cell patch clamp conditions[19].

In addition to inhibition by Mg^{2+}, TRPM7 is potently *inhibited* by μM concentrations of 2-Aminoethyl diphenylborinate (2-APB) and *potentiated* by mM concentrations of 2-APB; in contrast, 2-APB only potentiates TRPM6[20]. Consistent with this pharmacology, TRPM7-like currents measured from mouse cardiomyocytes were noted to be substantially inhibited by 200 μM 2-APB, but potentiated by 2.5 mM 2-APB (Figure 1E). Also, consistent with TRPM7, these currents were noted to exhibit the same dependence on external pH as previously described[21] (Figure 1F). Collectively, these data strongly suggest that the outwardly rectifying TRPM7-like current measured in mouse ventricular cardiomyocytes is indeed TRPM7.

Generation of cardiac-restricted TRPM7 deletion in myocardium

To circumvent the embryonic lethality associated with global deletion of *Trpm7*[9, 10], we generated mice with cardiac-restricted *Trpm7* deletion using Cre-loxP technology. The conditional *Trpm7* allele contained *loxP* sites flanking exon 17[10] (*Trpm7*$^{fl/fl}$). *Cre*-mediated recombination induces a frameshift that prevents expression of the ion channel and kinase domains of TRPM7[10]. We used a panel of *Cre*-expressing alleles that drive recombination at varying times in cardiac development (Figure 1G, see Methods): Islet1 (*Isl1-Cre*, ~E7[22], *Trpm7* $^{Isl1/fl}$), Troponin-T (*TnT-Cre*, ~E9[23], *Trpm7* $^{TnT/fl}$), and α-myosin heavy chain (α*MHC-Cre*, ~E12.5 [24], *Trpm7* $^{\alpha MHC/fl}$ and *Trpm7* $^{\alpha MHC/-}$).

We first evaluated α-*MHC-Cre* recombinase expression patterns by crossing *αMHC-Cre* mice with the *mT/mG* reporter mouse line (*ROSA26*^{mTmG}), in which membrane-targeted green fluorescent protein expression (mG) is induced only after *Cre*-mediated recombination[25]. *Cre* recombinase was expressed throughout the ventricular myocardium in a cardiomyocyte-restricted manner (Supplemental Figure 1A). Effective deletion of *Trpm7* exon 17 in myocardium is evident by PCR at postnatal day 1 in *Trpm7* $^{\alpha MHC/fl}$ mice (Supplemental Figure 1B) based on the presence of the expected size of the deletion product in cardiac genomic DNA. TRPM7 current is absent in enzymatically dissociated adult *Trpm7* $^{\alpha MHC/fl}$ cardiomyocytes (0.003 ± 0.03 pA/pF, n = 19 vs. 6.8± 0.8 pA/pF at +100 mV, n = 10 in *Trpm7*$^{fl/fl}$ (*WT*) myocytes; Figure 1H, I). These data confirm that TRPM7 protein is eliminated in *Trpm7* $^{\alpha MHC/fl}$ ventricular cardiomyocytes and establishes the identity of this Mg^{2+}-inhibitable outwardly rectifying current as TRPM7.

Trpm7 is required for early embryonic cardiac development but dispensable in adult myocardium

Based on our previous findings that TRPM7 was largely expressed in early embryonic myocardium[10], we examined the effects of *Trpm7* deletion at early (<E9, *Trpm7* $^{Isl1/fl}$, *Trpm7* $^{TnT/fl}$) and late (> E12.5, *Trpm7* $^{\alpha MHC/fl}$) stages of cardiac development. *TnT-Cre* recombines in the ventricle at approximately E9[23] (Supplemental Figure 1C) while *Isl1-Cre* recombines in the precursors of the secondary heart field (E7) that give rise to the right ventricle (RV) and right ventricular outflow tract[22] (Supplemental Figure 1D). *αMHC-Cre* deletes in ventricle at after E12.5[24]. We find no *Trpm7* $^{TnT/fl}$ or *Trpm7* $^{Isl1/fl}$ mice survive to birth. Deletion of *Trpm7* exon 17 in genomic DNA isolated from E9 *Trpm7* $^{TnT/fl}$ embryos confirms deletion at this time point (Supplemental Figure 1E). By embryonic day 10.5-11.5, both *Trpm7* $^{TnT/fl}$ and *Trpm7* $^{Isl1/fl}$ develop large pericardial effusions and blood congestion in the liver (Figure 2A, B; *TnT-Cre* shown), and die *in utero* of congestive heart failure by E11.5. Histological examination of E10.5-11 embryos reveals severe thinning of the compact myocardium and impaired ventricular septation in both genotypes (Figure 2C-F), with RV compact myocardium thinning predominant in *Trpm7* $^{Isl1/fl}$ embryos (Figure 2E). As thinned compact myocardium may result from either reduced proliferation or increased apoptosis, we next assessed cardiomyocyte proliferation by bromodeoxyuridine uptake (BrdU) and apoptosis by TUNEL assay. Immuno-stained *Trpm7* $^{TnT/fl}$ embryos show significantly reduced nuclear BrdU uptake in the compact myocardial layer as compared to *Trpm7* $^{TnT/+}$ controls (Figure 2G-I). In contrast, we detect no differences in myocyte apoptosis in *Trpm7* $^{TnT/fl}$ hearts compared to *Trpm7* $^{TnT/+}$ controls (Supplemental Figure 2), suggesting that impaired myocardial proliferation is the primary mechanism responsible for thinned myocardium and congestive heart failure upon early embryonic cardiac-targeted *Trpm7* deletion.

Remarkably, we find that all *Trpm7* $^{\alpha MHC/fl}$ mice survive to adulthood and exhibit entirely normal ventricular morphology and function, under basal conditions, as assessed in 4 to 6 week-old mice (Supplemental Table 1). These data suggest that *Trpm7* is critical for early events in embryonic cardiac development but is dispensable in late embryonic or adult myocardium.

The timing of cardiac TRPM7 deletion variably disrupts adult ventricular function, conduction and repolarization

To further probe the importance of *Trpm7* in the developmental period E9-E12.5, we generated an additional line of mice: *Trpm7* $^{\alpha MHC/-}$. This line is expected to delete *Trpm7* slightly earlier in embryonic development than *Trpm7* $^{\alpha MHC/fl}$, as there exists only one allele for *Cre*-mediated excision. Interestingly, this subtle difference in the timing of TRPM7 disruption results in significantly different cardiac phenotypes. *Trpm7* $^{\alpha MHC/-}$ mice exhibit a bimodal phenotype in which a subset of mice (12/30; 40%) develop a dilated cardiomyopathy (Figure 3A). This cardiomyopathy is associated with heart block (HB), as noted in the ECG during the echocardiogram (see Movies 1 and 2), and is independent of age. Heart weight: body weight ratios (Figure 3B), systolic function (Figure 3C), left ventricular size (Figure 3D) and calculated LV mass (Figure 3E) are all significantly abnormal in those *Trpm7* $^{\alpha MHC/-}$ mice with HB (*Trpm7* $^{\alpha MHC/-}$ *+HB*) as early as 3-4 weeks of age. *Trpm7* $^{\alpha MHC/-}$ mice without heart block (*Trpm7* $^{\alpha MHC/-}$ *−HB*) exhibit normal heart size, ventricular function and morphology (Figure 3AF, Movie 3). Isolation of ventricular myocytes from *TRPM7*$^{fl/fl}$ (*WT)* and *Trpm7* $^{\alpha MHC/-}$ *+HB* hearts confirm that cardiomegaly is due to cardiac myocyte hypertrophy (Figure 3G-H) as *Trpm7* $^{\alpha MHC/-}$ +HB myocytes are nearly two-fold larger by surface area ($Area_{WT}$ = 2002 ± 82 μm^2, n = 46; $Area_{Trpm7\alpha MHC/-\ +HB}$ = 3652 ± 176 μm^2, n = 49, p < 0.001; Figure 3I), and this increase in size is mediated primarily by an increase in myocyte length ($Length_{WT}$ = 101 ± 3.0 μm, n = 49;

Length $_{Trpm7}\alpha MHC/-_{+HB}$ = 163 ± 7.0 μm, n = 35, p < 0.001), while myocyte width is unchanged. This *eccentric* myocyte hypertrophy is consistent with the phenotype of dilated cardiomyopathy in *Trpm7* $^{\alpha MHC/-}$ hearts. In addition to cardiomyocyte hypertrophy, we also note significant interstitial extracellular matrix deposition and interstitial fibrosis on histological examination of *Trpm7* $^{\alpha MHC/-}$ hearts at 6-8 months of age (Supplemental Figure 3). Despite this pathology in *Trpm7* $^{\alpha MHC/-}$ mice, there is no significant difference in mortality observed out to 1 year of age as compared to littermate controls, including *Trpm7* $^{\alpha MHC/fl}$, *Trpm7* $^{\alpha MHC/+}$, and *Trpm7*$^{fl/fl}$ mice.

To better examine the electrophysiological defects in *Trpm7* $^{\alpha MHC/-}$ mice noted on echocardiography, we next performed sedated ECG's (Figure 4). We observe atrioventricular block in the same subset of mice with cardiomyopathy, ranging from second degree Mobitz Type 2 block with 2:1 conduction (Figure 4B), to 3:2/3:1 conduction (Figure 4C), to 5:1 conduction with coupled premature ventricular complexes (Figure 4D). Such severe heart block did not develop progressively, as it was evident in *Trpm7* $^{\alpha MHC/-}$ mice as early as 3-4 weeks of age with similar frequency (9/18; 50%). T waves are significantly flattened, and consequently QT intervals appear prolonged in normally conducted beats of the affected subpopulation of *Trpm7* $^{\alpha MHC/-}$ mice (Figure 4A, B-D, E). Furthermore, bidirectional ventricular arrhythmia can be reproducibly induced by precordial 'thump' in sedated *Trpm7* $^{\alpha MHC/-}$ mice with severe AV block and impaired ventricular repolarization (Figure 4F). Finally, ventricular arrhythmia is observed to occur spontaneously in some severely affected *Trpm7* $^{\alpha MHC/-}$ mice (Figure 4G, 4/12 mice; 33%). However, no sudden cardiac deaths occur in even the most severely affected mice.

Myocardial Mg^{2+} and Zn^{2+} are unchanged after *Trpm7* ablation

Since TRPM7 is known to permeate divalent cations and has been proposed to regulate intracellular magnesium[9] and zinc[26] homeostasis, it is possible that the phenotypes in *Trpm7* $^{\alpha MHC/-}$ mice arise from myocardial deficiencies of these divalents. To examine this possibility, we measured total cellular magnesium and zinc content (using Inductively-Coupled Mass Spectrometry; ICP-MS) in ventricular tissue from *Trpm7*$^{fl/fl}$ (*WT*), *Trpm7*$^{fl/-}$ and *Trpm7* $^{\alpha MHC/-}$ mice. We detect no differences in total cellular Mg^{2+} or Zn^{2+} between these groups (Supplemental Figure 4), confirming that neither myocardial hypomagnesemia nor hypozincemia occurs after cardiac-deletion of TRPM7, and thus are not associated with the cardiomyopathy or electrophysiological disorders observed in *Trpm7* $^{\alpha MHC/-}$ mice.

Microarray analysis of *Trpm7* $^{\alpha MHC/-}$ ventricular tissue

To search for putative pathways and biological processes induced by deletion of *Trpm7*, we performed microarray analysis on 3-5 week old *WT*, *Trpm7* $^{\alpha MHC/fl}$ and *Trpm7* $^{\alpha MHC/-}$ hearts. Strikingly, we found no significant transcriptional changes between *WT* and the later cardiac *Trpm7* knockout, *Trpm7* $^{\alpha MHC/fl}$ (Figure 5A). Conversely, we found that ~1300 genes were differentially expressed based on a criterion of at least a 1.3-fold change and an adjusted p-value < 0.05 when comparing *Trpm7* $^{\alpha MHC/-}$ to *WT* (Figure 5A, Supplemental Table 2). Fifteen differentially expressed genes of interest were then chosen to validate the microarray by qRTPCR (Figure 5B). Significant changes in gene expression are consistent with the phenotype of cardiac hypertrophy/ventricular remodeling *(Nppa, Acta1, Timp1, Postn)*, as well as electrical remodeling of both conduction system (*Trpm4, Hcn4, Kcnj3)*, and ventricular cells *(Kcnv2, Kcnd2, Kcnk3, Kcna1, Lgi1)*. Interestingly, pivotal transcriptional regulators of myocyte differentiation and cardiac hypertrophy (*Hdac5, Hdac9*) are also noted to be down-regulated. Using Gene Set Enrichment Analysis (GSEA, using http:// www.broadinstitute.org/gsea) we found *Trpm7* $^{\alpha MHC/-}$ hearts to be enriched in gene expression patterns pertaining to embryonic development, cellular proliferation and cellular differentiation pathways (Figure 5C; TGF-β1 response, SMAD6 targets, SMARCE1

target, PDGF signaling). Consistent with the phenotype of cardiomyopathy, we also observed the expected enrichment in genes up-regulated in the extracellular matrix (ECM), ECM receptor interactions, and pressure-overload murine heart disease. Genes downregulated in *Trpm7* $^{\alpha MHC/-}$ hearts compared to *WT* (or negative enrichments) clustered to metabolic pathways (tryptophan, fatty acid, lipid, peroxisome proliferator-activated receptor (PPAR) signaling) and mitochondrial function (Figure 5D).

Taken together, these findings show that cardiac phenotypes resulting from disruption of *Trpm7* arise primarily from perturbations in early embryonic ventricular development, not from altered global cellular Mg^{2+} or Zn^{2+} levels in adulthood, nor from a requirement of *Trpm7* in normal adult cardiomyocyte physiology, under basal conditions.

Trpm7 deletion silences *Hcn4* expression and I_f in atrioventricular node

To elucidate the molecular mechanism for atrioventricular block induced by cardiac *Trpm7* deletion we focused on ion channels downregulated in *Trpm7* $^{\alpha MHC/-}$ hearts that are enriched in atrioventricular node and are thought to be important for the normal activity of the cardiac conduction system. *Hcn4* encodes a hyperpolarization-activated cyclic nucleotide gated channel and is the predominant *Hcn* isoform in the cardiac conduction system. It is the primary molecular determinant of I_f and is important for pacemaking and atrioventricular node function. Indeed, inducible cardiac-targeted deletion of *Hcn4* in mouse results in severe heart block[27]. We measured the I_f current in freshly isolated atrioventricular node (AVN) cells from *WT* and *Trpm7* $^{\alpha MHC/-}$ *+HB* hearts by whole-cell patch clamp (Figure 6, **inset**) to determine whether reductions in *Hcn4* mRNA from whole ventricle reflect reductions in I_f current in AVN. We find robust I_f currents in all AVN cells isolated from *WT* mice ($I_{f,\ WT}$ = −32.6 ± 7.3 pA/pF at −160 mV, n = 9) (Figure 6A, **left, B,C**). In *Trpm7* $^{\alpha MHC/-}$ *+HB* hearts, I_f is on average significantly diminished in AVN cells ($I_{f,\ Trpm7\alpha MHC/-\ +HB}$ = −7.3 ± 2.7 pA/pF at −160 mV, n = 15; Figure 6B, C), and remarkably absent in some (6/15) (Figure 6A, **center**). Notably, of the subset of AVN cells from *Trpm7* $^{\alpha MHC/-}$ *+HB* with measurable I_f, a few have significantly increased activation kinetics (Figure 6A, **right**), which is suggestive of I_f encoded by *Hcn2* and/or *Hcn1*[28]. Since *Hcn1*, *Hcn2* and *Hcn4* all contribute to I_f in heart, down regulation of *Hcn4* is anticipated to uncover the component of I_f provided by *Hcn1* and *Hcn2*, as seen previously in an *Hcn4* knockout model[29]. Taken together these data suggest that deletion of *Trpm7* in heart suppresses *Hcn4* expression and I_f current in AVN cells resulting in atrioventricular block.

Trpm7 deletion prolongs action potentials in ventricular cells via reductions in transient outward current

The T wave flattening on sedated ECGs of *Trpm7* $^{\alpha MHC/-}$ mice suggests a defect in ventricular repolarization. Transcriptional analysis of *Trpm7* $^{\alpha MHC/-}$ ventricular tissue revealed significant down-regulation of numerous potassium channel genes (*Kcnd2, Kcnk3, Kcna1)* and potassium channel modifier genes (*Kcnv2, Lgi1)* [30, 31]. Of these genes, *Kcnd2,* encoding the transient outward current (I_{to}), is the most prominent outward current in murine ventricular cells[32], dominating ventricular repolarization[33]. Indeed, eliminating I_{to} or its transmural gradient in mouse is sufficient to induce QT prolongation, T wave flattening and triggered ventricular tachycardia[34]. Accordingly, we measured I_{to} in freshly dissociated ventricular myocytes from *WT* and *Trpm7* $^{\alpha MHC/-}$ *+HB.* We find that total peak outward potassium current (I_{peak}) and I_{to} ($I_{peak} - I_{sus}$, see Methods) measured at +60 mV is significantly diminished in *Trpm7* $^{\alpha MHC/-}$ *+HB* ventricular cells ($I_{peak\text{-}LV,\ Trpm7\alpha MHC/-\ +HB}$ = 11 ± 0.9 pA/pF, n = 12; $I_{to\text{-}LV,\ Trpm7\alpha MHC/-\ +HB}$ = 5 ± 0.9 pA/pF, n = 12) compared to *WT* ($I_{peak\text{-}LV,\ WT}$ = 26 ± 2.4 pA/pF, n = 29; $I_{to\text{-}LV,\ WT}$ = 19 ± 2.1, n = 29, p <0.001) (Figure 7A&B). The sustained component, I_{sus}, contributed by delayed rectifiers[32] is not different ($I_{sus\text{-}LV,\ WT}$ = 7 ± 0.4 pA/pF, n = 29; $I_{sus\text{-}LV,\ Trpm7\alpha MHC/-\ +HB}$ = 6 ± 0.3

pA/pF, n = 12, p = 0.1), supporting the notion that the transient outward currents specifically, and not all outward potassium currents, are diminished in *Trpm7* $^{\alpha MHC/-}$ *+HB* myocytes. Furthermore, the broad distribution of I_{peak} and I_{to} current densities observed in ventricular myocytes from *WT* hearts, reflecting the normal transmural gradient of I_{to}, appears to be abolished in *Trpm7* $^{\alpha MHC/-}$ *+HB* hearts (Figure 7B). As a result of I_{to} down regulation, action potentials (AP) measured in *Trpm7* $^{\alpha MHC/-}$ *+HB* myocytes from both LV and RV are significantly prolonged compared to *WT* (Figure 7C, Table 1). Furthermore, in a number of *Trpm7* $^{\alpha MHC/-}$ *+HB* myocytes with prolonged APs, early afterdepolarizations (EAD) are observed (Figure 7D). These EADs may provide triggers for spontaneous ventricular arrhythmias observed in *Trpm7* $^{\alpha MHC/-}$ *+HB* mice (Figure 3G). As TRPM7 mediates an outward current at depolarized membrane potentials (0 to +50 mV), it is possible that this may contribute directly to AP repolarization. However, in Figure 1 we showed that prior to myocyte dialysis, TRPM7 current ("break-in" current) is inactive under basal conditions. Indeed, consistent with this notion, under physiological conditions, we find that *Trpm7* $^{\alpha MHC/fl}$ ventricular AP properties are not different from WT (Table 1). These data suggest that TRPM7 contributes minimally in a *direct* fashion to AP repolarization under basal conditions. Instead, the pronounced AP changes seen in *Trpm7* $^{\alpha MHC/-}$ myocytes result *indirectly* from reductions in *Kcnd2* expression and I_{to}. Taken together, these results establish a cellular mechanism for both the impairment in ventricular repolarization and ventricular tachycardia observed in *Trpm7* $^{\alpha MHC/-}$ mice (Figure 3).

Since down regulation of *Kcnd2* and I_{to} are well known to occur in the setting of cardiac hypertrophy[33], it is possible that these effects of *Trpm7* deletion on *Kcnd2* expression, I_{to} current and myocyte repolarization may be secondary to the hypertrophic response. To dissect out the contributions of cardiac hypertrophy from the effects of *Trpm7* deletion on myocardial gene expression we next examined, by qRT-PCR, expression levels of the same subset of differentially expressed genes in *Trpm7* $^{\alpha MHC/-}$ mice *without* heart block (*Trpm7* $^{\alpha MHC/-}$ *−HB*) since these hearts are not hypertrophied (Figure 8A). Consistent with the absence of cardiac hypertrophy in these *Trpm7* $^{\alpha MHC/-}$ *−HB* mice, hypertrophy/remodeling genes previously increased in *Trpm7* $^{\alpha MHC/-}$ *+HB* are largely unchanged, with the exception of *Timp1,* which remains significantly elevated. Also, *Hcn4* expression in *Trpm7* $^{\alpha MHC/-}$ *−HB* hearts is unchanged, consistent with the absence of AV block in these hearts. Remarkably, many of the potassium channel genes (*Kcnj3, Kcnd2*), channel modifier genes (*Kcnv2*, *Lgi1*), *Trpm4*, and *Hdac9* remain significantly down regulated.

We patch-clamped freshly isolated ventricular myocytes from *Trpm7* $^{\alpha MHC/-}$ *−HB* hearts to determine whether these reductions in *Kcnd2* expression in whole heart translated to reduced I_{to} and impaired AP repolarization. We find I_{to} to be significantly reduced in *Trpm7* $^{\alpha MHC/-}$ *−HB* ventricular myocytes ($I_{to\text{-}LV,\ Trpm7\alpha MHC/-\ -HB}$ = 11 ± 2.1 pA/pF, n = 20) compared to WT ($I_{to\text{-}LV,\ WT}$ = 19 ± 2.1, n = 29, P <0.05; Figure 8B, **center**), but to a lesser extent than observed in *Trpm7* $^{\alpha MHC/-}$ *+HB* myocytes ($I_{to\text{-}LV,\ Trpm7\alpha MHC/-\ +HB}$ = 5 ± 0.9 pA/pF, n = 12). Importantly, cell capacitance measurements (Figure 8B, **right**), which are proportional to cell surface area, confirm that *Trpm7* $^{\alpha MHC/-}$ *−HB* myocytes are not hypertrophied ($Cap_{\ Trpm7\alpha MHC/-\ -HB}$ = 103 ± 7 pF, n = 22), but are instead significantly smaller than *WT* myocytes (Cap_{WT} = 168 ± 9 pF, n = 29, p < 0.001). Examining the distribution of I_{peak} and I_{to} amplitudes in *Trpm7* $^{\alpha MHC/-}$ *−HB* myocytes (Figure 8B, **dotted black and red circles**) reveals a bimodal distribution suggestive of a mosaic effect on I_{to} down regulation in these hearts. The distribution of I_{to} current densities from *Trpm7* $^{\alpha MHC/-}$ *−HB* ventricular cells is best fit by two Gaussian distributions (R^2 = 1), with one population centered at 5 pA/pF and another centered at 25 pA/pF (Supplemental Figure 5). On the other hand, the distribution of *WT* I_{to} current densities is best fit by a single Gaussian (R^2 = 0.99). The mean I_{to} current density in the subgroup of ventricular myocytes from *Trpm7* $^{\alpha MHC/-}$ *−HB* hearts with lower I_{to} ($I_{to\text{-}red\ circle,}$ = 7 ± 1.1 pA/pF, n = 15) is significantly different from the other group

($I_{to\text{-}black\ circle}$ = 25 ± 1.6, n = 6, P < 0.001) and comparable to I_{to} from *Trpm7* $^{\alpha MHC/-}$ *+HB* myocytes ($I_{to\text{-}LV,\ Trpm7\alpha MHC/-\ +HB}$ = 5 ± 0.9 pA/pF, n = 12, p = 0.2). This mosaic effect is also reflected in the APs measured from *Trpm7* $^{\alpha MHC/-}$ *−HB* ventricular myocytes as these ranged from *WT*-like in a small subset (Figure 8C, **left**) to markedly prolonged (Figure 8C, **right**). Nonetheless, the mean AP durations measured in *Trpm7* $^{\alpha MHC/-}$ *−HB* myocytes (APD_{50} = 20 ± 8.0 ms, n = 18) are comparable to *Trpm7* $^{\alpha MHC/-}$ *+HB* (APD_{50} = 22 ± 7.0 ms, n = 19) and significantly longer than *WT* ($APD_{50,\ WT}$ = 6 ± 0.8 ms, n = 33, p < 0.01; Table 1).

DISCUSSION

We sought to determine the contribution of TRPM7 to cardiac function by studying the consequences of cardiac-targeted *Trpm7* deletion. By examining phenotypes resulting from *Trpm7* deletion at different time-points in cardiogenesis using a panel of cardiac-targeted *Cre* lines (*Isl1-Cre*, ~E7; *TnT-Cre*, ~E9; *αMHC-Cre*, ~E12.5) we show that the timing of *Trpm7* deletion variably perturbs cardiac development and function. Late embryonic deletion (*αMHC-Cre*) results in normal ventricular function, while early embryonic deletion (*Isl1-Cre*/*TnT-Cre)*, leads to impaired compact myocardium development with consequent congestive heart failure and embryonic death. Deletion of *Trpm7* between these two time points in cardiogenesis results in a ~50% penetrant adult cardiomyopathy characterized by ventricular dysfunction, disrupted atrioventricular conduction, dispersed ventricular repolarization and spontaneous/inducible ventricular arrhythmias (Supplemental Figure 6). This cardiomyopathy is associated with up-regulated hypertrophy/remodeling genes (*Nppa/ Acta1/Postn/TGF-ß2/Timp1*) while repolarizing potassium channel genes *(Kcnk3, Kcna1, Kcnd2, Kcnj3, Kcnv2)* and genes expressed in the conduction system (*Trpm4, Hcn4, Kcnj3*) are down regulated. This phenotype does not arise from dysregulated myocardial magnesium levels, as we observe no changes in total intracellular magnesium (or zinc) content in TRPM7-deficient myocardium, consistent with our previous findings in *Trpm7* deleted T-lymphocytes[10], or in other tissues[11]. These data further support the contention that, in adult tissue, TRPM7 is not required for magnesium homeostasis[10, 11]. Alternative magnesium influx pathways (*e.g.*, MagT1, TUSC3, ACDP/CNNM, other TRPM channels, CNG channels) are likely more important or able to compensate loss of TRPM7 to determine global intracellular magnesium levels in adult tissue[35, 36].

The dilated cardiomyopathy that occurs with cardiac-targeted TRPM7 deletion appears associated with heart block and therefore suggests that this cardiomyopathy may arise from hemodynamic stresses secondary to chronic bradycardia rather than from primary effects of *Trpm7* deletion. On the other hand, it is notable that both heart block and cardiomyopathy are observed concomitantly in *Trpm7* $^{\alpha MHC/-}$ mice as early as 3 weeks of age, and the extent of left ventricular remodeling/dysfunction does not correlate with the severity of heart block. This argues against a mechanism of chronic bradycardia-induced cardiomyopathy and suggests, instead, that this phenotype is congenital in nature or very rapidly progressing. The finding that histone deacetlyase 9 (*Hdac9*) and to a lesser extent histone deacetlyase 5 (*Hdac5*) are downregulated in all in *Trpm7* $^{\alpha MHC/-}$ mice could provide a mechanism for a rapidly progressive cardiomyopathy in the context of only mild heart block. HDAC5/9 have been shown to act as transcriptional repressors of myocyte enhancing factor 2c (Mef2c), a critical transcription factor mediating gene expression in cardiac development[37] and hypertrophy [38]. Indeed, *HDAC9*$^{-/-}$ mice develop exaggerated cardiac hypertrophy when subjected to pressure-overload or chronic calcineurin activation [38]. It is possible that HDAC5/9 down regulation in *Trpm7* $^{\alpha MHC/-}$ mice may sensitize the heart to cardiac hypertrophy such that a normally innocuous hemodynamic challenge (mild heart block) can induce a significant cardiomyopathy.

Atrioventricular (AV) block observed with cardiac-targeted *Trpm7* deletion is associated with significant down regulation of a hyperpolarization-activated cyclic nucleotide gated channel gene (*Hcn4*) and a transient receptor potential channel gene (*Trpm4*). Both *Hcn4* and *Trpm4* are expressed in the murine and human atrioventricular node and conduction system [4, 39]. Mutations in *Trpm4* have been associated with progressive familial heart block type 1 (PFHBI) in humans[4] and inducible cardiac-targeted deletion of *Hcn4* in mouse results in severe heart block[27]. Indeed, we find that the I_f current encoded by *Hcn4* is significantly depressed and often entirely silenced in AVN cells from *Trpm7* $^{\alpha MHC/-}$ *+HB* mice, providing a cellular mechanism for HB in these mice.

In addition to heart block, *Trpm7* $^{\alpha MHC/-}$ mice exhibit T wave flattening suggestive of impaired ventricular repolarization, associated with reduced expression of numerous potassium channel genes, including *Kcnd2*. *Kcnd2* encodes the transient outward current (I_{to}), which is the primary repolarizing current in rodents[33], and when selectively eliminated in mice results in QT prolongation, atrioventricular block, early-after-depolarizations and ventricular tachycardia[40, 41]. Similarly, elimination of I_{to} by deleting Kv Channel Interacting Protein 2 (KChiP2) also confers susceptibility to ventricular tachycardia[42], as does loss of the transmural I_{to} gradient due to knock-out of the homeodomain transcription factor Irx5[34]. We find that I_{to} is significantly diminished in patch-clamped *Trpm7* $^{\alpha MHC/-}$ ventricular cells and consequently action potentials are considerably prolonged compared to *WT*.

In summary, we show that the mechanisms responsible for TRPM7-mediated effects on cardiac function are complex. They result from changes in myocardial transcription that depends on the level of TRPM7 in myocardium during early developmental events, rather than on a direct role of TRPM7 in cardiac function (Supplemental Figure 6). The notion that altered cardiac function in adult mice arise from perturbations in *Trpm7* activity during embryonic development is a novel and unique concept among TRP channels and is also consistent with our findings in other tissues[11]. Our efforts are now focused on elucidating how this ion channel-kinase is able to transduce changes in gene expression to influence cellular differentiation/development in a timing-dependent fashion. One important direction centers on our recently published finding that TRPM7 carboxy-terminal kinase can be cleaved from the ion channel in lymphocytes and activate down-stream signaling events[43]. Indeed, we find that a significant amount of TRPM7 is cleaved in embryonic myocardium compared to adult myocardium (RS, GK, DEC, unpublished observations). We speculate that these cleavage fragments may be interacting, either directly, or indirectly, with key cardiac transcription factors important for myocardial development and cardiac hypertrophy (e.g. Mef2). Furthermore, given the extent of cardiac pathology that ensues from disruptions in TRPM7 function, it is possible that patients with unexplained structural or electrophysiological heart disease may harbor previously unidentified disease causing mutations in *Trpm7*.

Supplementary Material

Refer to Web version on PubMed Central for supplementary material.

Acknowledgments

We thank Janice L. Robertson for assistance with data analysis and her thoughtful review of the manuscript.

Funding Sources: This work was supported by the Howard Hughes Medical Institute (HHMI, DEC), the Leadership Council in Cardiovascular Care (LCIC, RS) and the American Heart Association (AHA) Fellow-to-Faculty transition award (RS). Microarray studies were performed by the Molecular Genetics Core Facility at Children's Hospital Boston (NIH-P50-NS40828, and NIH-P30-HD18655). Mice generated by Neurodevelopmental Behavioral Core and the Gene Manipulation Facility of the Boston Children's Hospital Mental Retardation and Developmental Disabilities Research Center (NIH grant P30-HD18655). DC was supported by the NIH grant

F32HL107021. ANR-2010-BLAN-1128-01 and ANR-09-GENO-034 (MEM). The IGF group is a member of the Laboratory of Excellence, Ion Channel Science and Therapeutics and is supported by a grant from ANR.

References

1. Kuwahara K, Wang Y, McAnally J, Richardson JA, Bassel-Duby R, Hill JA, Olson EN. Trpc6 fulfills a calcineurin signaling circuit during pathologic cardiac remodeling. J Clin Invest. 2006; 116:3114–3126. [PubMed: 17099778]
2. Wu X, Eder P, Chang B, Molkentin JD. Trpc channels are necessary mediators of pathologic cardiac hypertrophy. Proc Natl Acad Sci U S A. 2010; 107:7000–7005. [PubMed: 20351294]
3. Satoh S, Tanaka H, Ueda Y, Oyama J, Sugano M, Sumimoto H, Mori Y, Makino N. Transient receptor potential (trp) protein 7 acts as a g protein-activated ca2+ channel mediating angiotensin ii-induced myocardial apoptosis. Mol Cell Biochem. 2007; 294:205–215. [PubMed: 16838106]
4. Kruse M, Schulze-Bahr E, Corfield V, Beckmann A, Stallmeyer B, Kurtbay G, Ohmert I, Brink P, Pongs O. Impaired endocytosis of the ion channel trpm4 is associated with human progressive familial heart block type i. J Clin Invest. 2009; 119:2737–2744. [PubMed: 19726882]
5. Liu H, El Zein L, Kruse M, Guinamard R, Beckmann A, Bozio A, Kurtbay G, Megarbane A, Ohmert I, Blaysat G, Villain E, Pongs O, Bouvagnet P. Gain-of-function mutations in trpm4 cause autosomal dominant isolated cardiac conduction disease. Circ Cardiovasc Genet. 2010; 3:374–385. [PubMed: 20562447]
6. Guinamard R, Demion M, Magaud C, Potreau D, Bois P. Functional expression of the trpm4 cationic current in ventricular cardiomyocytes from spontaneously hypertensive rats. Hypertension. 2006; 48:587–594. [PubMed: 16966582]
7. Mathar I, Vennekens R, Meissner M, Kees F, Van der Mieren G, Camacho Londono JE, Uhl S, Voets T, Hummel B, van den Bergh A, Herijgers P, Nilius B, Flockerzi V, Schweda F, Freichel M. Increased catecholamine secretion contributes to hypertension in trpm4-deficient mice. J Clin Invest. 2010; 120:3267–3279. [PubMed: 20679729]
8. Bates-Withers C, Sah R, Clapham DE. Trpm7, the mg(2+) inhibited channel and kinase. Adv Exp Med Biol. 2011; 704:173–183. [PubMed: 21290295]
9. Ryazanova LV, Rondon LJ, Zierler S, Hu Z, Galli J, Yamaguchi TP, Mazur A, Fleig A, Ryazanov AG. Trpm7 is essential for mg(2+) homeostasis in mammals. Nat Commun. 2010; 1:109. [PubMed: 21045827]
10. Jin J, Desai BN, Navarro B, Donovan A, Andrews NC, Clapham DE. Deletion of trpm7 disrupts embryonic development and thymopoiesis without altering mg2+ homeostasis. Science. 2008; 322:756–760. [PubMed: 18974357]
11. Jin J, Wu LJ, Jun J, Cheng X, Xu H, Andrews NC, Clapham DE. The channel kinase, trpm7, is required for early embryonic development. Proc Natl Acad Sci U S A. 2012; 109:E225–233. [PubMed: 22203997]
12. Kunert-Keil C, Bisping F, Kruger J, Brinkmeier H. Tissue-specific expression of trp channel genes in the mouse and its variation in three different mouse strains. BMC Genomics. 2006; 7:159. [PubMed: 16787531]
13. Fonfria E, Murdock PR, Cusdin FS, Benham CD, Kelsell RE, McNulty S. Tissue distribution profiles of the human trpm cation channel family. J Recept Signal Transduct Res. 2006; 26:159–178. [PubMed: 16777713]
14. Du J, Xie J, Zhang Z, Tsujikawa H, Fusco D, Silverman D, Liang B, Yue L. Trpm7-mediated ca2+ signals confer fibrogenesis in human atrial fibrillation. Circ Res. 2010; 106:992–1003. [PubMed: 20075334]
15. Aarts M, Iihara K, Wei WL, Xiong ZG, Arundine M, Cerwinski W, MacDonald JF, Tymianski M. A key role for trpm7 channels in anoxic neuronal death. Cell. 2003; 115:863–877. [PubMed: 14697204]
16. Runnels LW, Yue L, Clapham DE. The trpm7 channel is inactivated by pip(2) hydrolysis. Nat Cell Biol. 2002; 4:329–336. [PubMed: 11941371]
17. Gwanyanya A, Sipido KR, Vereecke J, Mubagwa K. Atp and pip2 dependence of the magnesium-inhibited, trpm7-like cation channel in cardiac myocytes. Am J Physiol Cell Physiol. 2006; 291:C627–635. [PubMed: 16707555]

18. Demeuse P, Penner R, Fleig A. Trpm7 channel is regulated by magnesium nucleotides via its kinase domain. J Gen Physiol. 2006; 127:421–434. [PubMed: 16533898]
19. Langeslag M, Clark K, Moolenaar WH, van Leeuwen FN, Jalink K. Activation of trpm7 channels by phospholipase c-coupled receptor agonists. J Biol Chem. 2007; 282:232–239. [PubMed: 17095511]
20. Li M, Jiang J, Yue L. Functional characterization of homo- and heteromeric channel kinases trpm6 and trpm7. J Gen Physiol. 2006; 127:525–537. [PubMed: 16636202]
21. Jiang J, Li M, Yue L. Potentiation of trpm7 inward currents by protons. J Gen Physiol. 2005; 126:137–150. [PubMed: 16009728]
22. Laugwitz KL, Moretti A, Lam J, Gruber P, Chen Y, Woodard S, Lin LZ, Cai CL, Lu MM, Reth M, Platoshyn O, Yuan JX, Evans S, Chien KR. Postnatal isl1+ cardioblasts enter fully differentiated cardiomyocyte lineages. Nature. 2005; 433:647–653. [PubMed: 15703750]
23. Chen JW, Zhou B, Yu QC, Shin SJ, Jiao K, Schneider MD, Baldwin HS, Bergelson JM. Cardiomyocyte-specific deletion of the coxsackievirus and adenovirus receptor results in hyperplasia of the embryonic left ventricle and abnormalities of sinuatrial valves. Circ Res. 2006; 98:923–930. [PubMed: 16543498]
24. Gaussin V, Van de Putte T, Mishina Y, Hanks MC, Zwijsen A, Huylebroeck D, Behringer RR, Schneider MD. Endocardial cushion and myocardial defects after cardiac myocyte-specific conditional deletion of the bone morphogenetic protein receptor alk3. Proc Natl Acad Sci U S A. 2002; 99:2878–2883. [PubMed: 11854453]
25. Muzumdar MD, Tasic B, Miyamichi K, Li L, Luo L. A global double-fluorescent cre reporter mouse. Genesis. 2007; 45:593–605. [PubMed: 17868096]
26. Inoue K, Branigan D, Xiong ZG. Zinc-induced neurotoxicity mediated by transient receptor potential melastatin 7 channels. J Biol Chem. 2010; 285:7430–7439. [PubMed: 20048154]
27. Baruscotti M, Bucchi A, Viscomi C, Mandelli G, Consalez G, Gnecchi-Rusconi T, Montano N, Casali KR, Micheloni S, Barbuti A, DiFrancesco D. Deep bradycardia and heart block caused by inducible cardiac-specific knockout of the pacemaker channel gene hcn4. Proc Natl Acad Sci U S A. 2011; 108:1705–1710. [PubMed: 21220308]
28. Robinson RB, Siegelbaum SA. Hyperpolarization-activated cation currents: From molecules to physiological function. Annu Rev Physiol. 2003; 65:453–480. [PubMed: 12471170]
29. Herrmann S, Stieber J, Stockl G, Hofmann F, Ludwig A. Hcn4 provides a ‘depolarization reserve’ and is not required for heart rate acceleration in mice. Embo J. 2007; 26:4423–4432. [PubMed: 17914461]
30. Czirjak G, Toth ZE, Enyedi P. Characterization of the heteromeric potassium channel formed by kv2.1 and the retinal subunit kv8.2 in xenopus oocytes. J Neurophysiol. 2007; 98:1213–1222. [PubMed: 17652418]
31. Schulte U, Thumfart JO, Klocker N, Sailer CA, Bildl W, Biniossek M, Dehn D, Deller T, Eble S, Abbass K, Wangler T, Knaus HG, Fakler B. The epilepsy-linked lgi1 protein assembles into presynaptic kv1 channels and inhibits inactivation by kvbeta1. Neuron. 2006; 49:697–706. [PubMed: 16504945]
32. Guo W, Xu H, London B, Nerbonne JM. Molecular basis of transient outward k+ current diversity in mouse ventricular myocytes. J Physiol. 1999; 521(Pt 3):587–599. [PubMed: 10601491]
33. Oudit GY, Kassiri Z, Sah R, Ramirez RJ, Zobel C, Backx PH. The molecular physiology of the cardiac transient outward potassium current (i(to)) in normal and diseased myocardium. J Mol Cell Cardiol. 2001; 33:851–872. [PubMed: 11343410]
34. Costantini DL, Arruda EP, Agarwal P, Kim KH, Zhu Y, Zhu W, Lebel M, Cheng CW, Park CY, Pierce SA, Guerchicoff A, Pollevick GD, Chan TY, Kabir MG, Cheng SH, Husain M, Antzelevitch C, Srivastava D, Gross GJ, Hui CC, Backx PH, Bruneau BG. The homeodomain transcription factor irx5 establishes the mouse cardiac ventricular repolarization gradient. Cell. 2005; 123:347–358. [PubMed: 16239150]
35. Zhou H, Clapham DE. Mammalian magt1 and tusc3 are required for cellular magnesium uptake and vertebrate embryonic development. Proc Natl Acad Sci U S A. 2009; 106:15750–15755. [PubMed: 19717468]

36. Li FY, Chaigne-Delalande B, Kanellopoulou C, Davis JC, Matthews HF, Douek DC, Cohen JI, Uzel G, Su HC, Lenardo MJ. Second messenger role for mg2+ revealed by human t-cell immunodeficiency. Nature. 2011; 475:471–476. [PubMed: 21796205]
37. Chang S, McKinsey TA, Zhang CL, Richardson JA, Hill JA, Olson EN. Histone deacetylases 5 and 9 govern responsiveness of the heart to a subset of stress signals and play redundant roles in heart development. Mol Cell Biol. 2004; 24:8467–8476. [PubMed: 15367668]
38. Zhang CL, McKinsey TA, Chang S, Antos CL, Hill JA, Olson EN. Class ii histone deacetylases act as signal-responsive repressors of cardiac hypertrophy. Cell. 2002; 110:479–488. [PubMed: 12202037]
39. Herrmann S, Layh B, Ludwig A. Novel insights into the distribution of cardiac hcn channels: An expression study in the mouse heart. J Mol Cell Cardiol. 2011; 51:997–1006. [PubMed: 21945247]
40. Guo W, Li H, London B, Nerbonne JM. Functional consequences of elimination of i(to,f) and i(to,s): Early afterdepolarizations, atrioventricular block, and ventricular arrhythmias in mice lacking kv1.4 and expressing a dominant-negative kv4 alpha subunit. Circ Res. 2000; 87:73–79. [PubMed: 10884375]
41. London B, Baker LC, Petkova-Kirova P, Nerbonne JM, Choi BR, Salama G. Dispersion of repolarization and refractoriness are determinants of arrhythmia phenotype in transgenic mice with long qt. J Physiol. 2007; 578:115–129. [PubMed: 17110412]
42. Kuo HC, Cheng CF, Clark RB, Lin JJ, Lin JL, Hoshijima M, Nguyen-Tran VT, Gu Y, Ikeda Y, Chu PH, Ross J, Giles WR, Chien KR. A defect in the kv channel-interacting protein 2 (kchip2) gene leads to a complete loss of i(to) and confers susceptibility to ventricular tachycardia. Cell. 2001; 107:801–813. [PubMed: 11747815]
43. Desai BN, Krapivinsky G, Navarro B, Krapivinsky L, Carter BC, Febvay S, Delling M, Penumaka A, Ramsey IS, Manasian Y, Clapham DE. Cleavage of trpm7 releases the kinase domain from the ion channel and regulates its participation in fas-induced apoptosis. Dev Cell. 2012; 22:1149–1162. [PubMed: 22698280]
44. Sah R, Oudit GY, Nguyen TT, Lim HW, Wickenden AD, Wilson GJ, Molkentin JD, Backx PH. Inhibition of calcineurin and sarcolemmal ca2+ influx protects cardiac morphology and ventricular function in k(v)4.2n transgenic mice. Circulation. 2002; 105:1850–1856. [PubMed: 11956130]

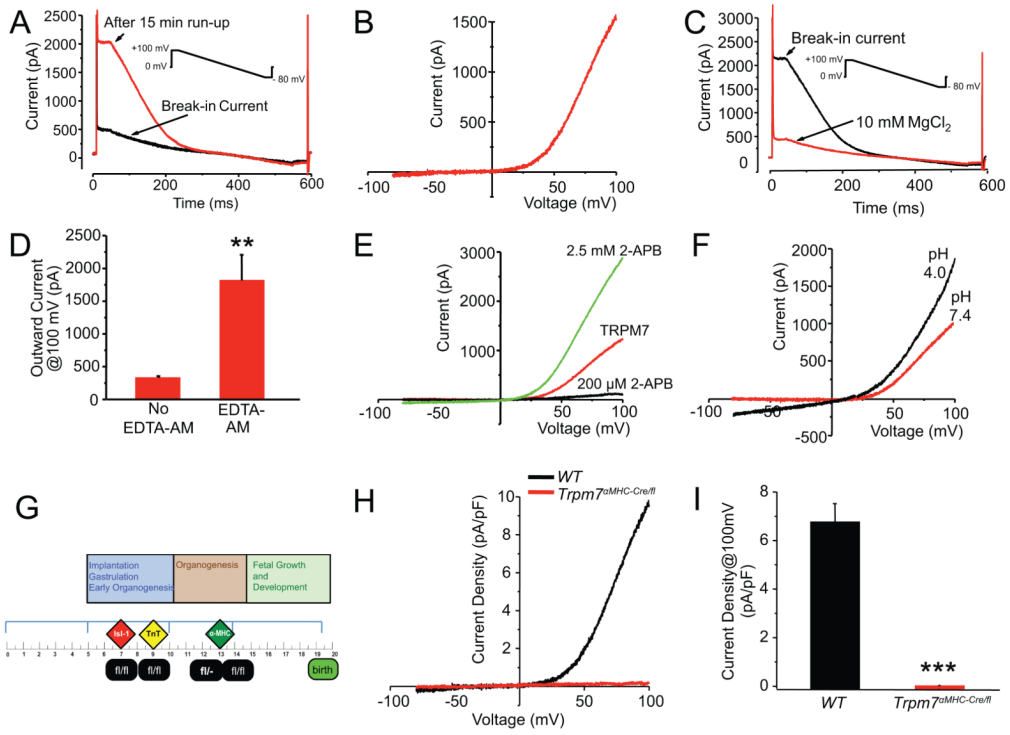

Figure 1.

Trpm7 current in freshly isolated mouse ventricular myocytes. **(A)** Current vs. time in response to 500 ms voltage ramp from +100 mV to −80 mV (after the initial 40 ms at +100 mV). *Black trace;* initial current immediately after establishing whole-cell configuration (break-in current). Over the course of 15 min, an outwardly rectifying current develops (*red trace*). **(B)** Characteristic outwardly-rectifying TRPM7 current trace derived from subtraction of break-in current (or current in 10 mM $MgCl_2$, as in **C**) from the steady-state current that develops after ~15 min. **(C)** Break-in current measured from a mouse ventricular myocyte after incubation in 30 μM EDTA-AM for 30 min (*black trace*) and after application of 10 mM $MgCl_2$ (*red trace*). **(D)** Mean outward current at +100 mV on break-in with (1813 ± 394 pA, n = 5) and without (327 ± 28 pA, n = 7) 30 μM EDTA-AM incubation. **(E)** Response of TRPM7-like current (*red*) to 200 μM (*black*) and 2.5 mM (*green*) 2-APB. **(F)** Potentiation of TRPM7-like current by low extracellular pH. **(G)** A panel of *Cre*-expressing alleles was used to drive recombination at varying times in cardiac development: Islet1 (*Isl1-Cre*), Troponin-T (*TnT-Cre*), and α-myosin heavy chain (*αMHC-Cre*). **(H, I)** *Trpm7* current is eliminated in all *Trpm7* $^{\alpha MHC/fl}$ ventricular myocytes compared to *WT*. Mean current densities at +100 mV, in *Trpm7* $^{\alpha MHC/fl}$ and *WT* myocytes. ** $p < 0.01$, *** $p < 0.001$.

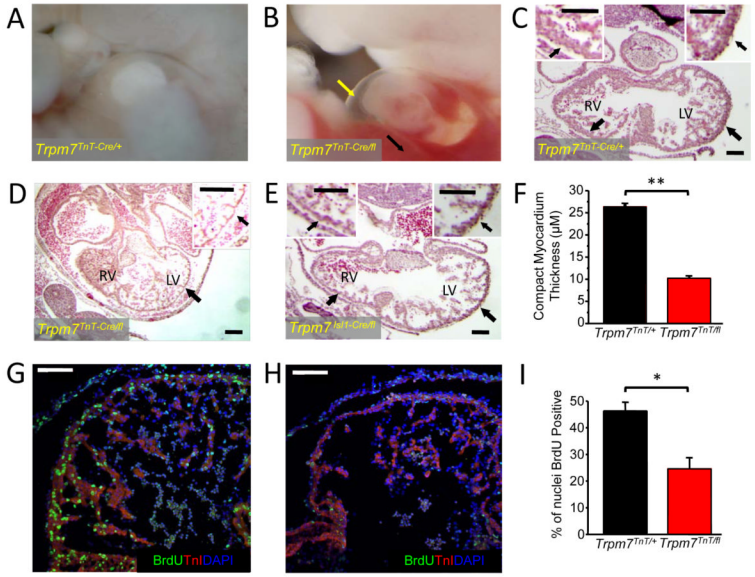

Figure 2.

Trpm7$^{TnT/fl}$ and *Trpm7*$^{Isl1/fl}$ mice develop severe thinning of the compact myocardium and die of congestive heart failure *in utero.* E10.5 WT embryo **(A)** compared with age-matched *Trpm7*$^{TnT/fl}$ embryo **(B)**. Note pericardial effusions (*yellow arrow*) and hepatic congestion (*black arrow*) consistent with congestive heart failure in E10.5 *Trpm7*$^{TnT/fl}$ mice. Hematoxylin-Eosin stain of *Trpm7 Trpm7*$^{TnT/+}$ **(C)**, *Trpm7*$^{TnT/fl}$ **(D)** and *Trpm7*$^{Isl1/fl}$ **(E)** heart sections. *Trpm7*$^{TnT/fl}$ and *Trpm7*$^{Isl1/fl}$ hearts show severe thinning of the compact myocardium **(D, E, black arrows)**. Insets in **C-E** show expanded views of right and left ventricular walls (RV and LV). **(F)** Mean data of compact myocardium thickness in *Trpm7*$^{TnT/+}$ (n = 188, from 3 hearts) and *Trpm7*$^{TnT/fl}$ (n = 300, from 3 hearts). Heart cryosections from **(G)** *Trpm7*$^{TnT/+}$ and **(H)** *Trpm7*$^{TnT/fl}$ embryos immunostained with cardiac Troponin-I (*TnI: red)* and bromodeoxyuridine (BrdU: green). Nuclei stained with DAPI (*blue*). **(I)** Percent of BrdU positive nuclei are significantly reduced in *Trpm7*$^{TnT/fl}$ compared to *Trpm7*$^{TnT/+}$ controls (n = 4 hearts each). Scale bar, 100 μm. * $p < 0.05$, ** $p < 0.01$.

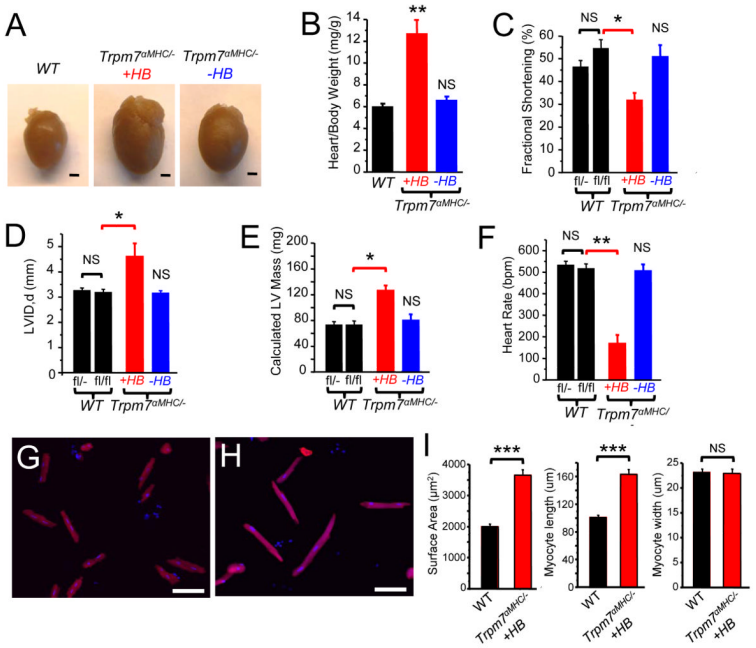

Figure 3.

Dilated cardiomyopathy in *Trpm7* $^{\alpha MHC/-}$ mice. **(A)** Hearts extracted from *Trpm7*$^{fl/fl}$*(WT)* and *Trpm7* $^{\alpha MHC/-}$ mice with heart block (*+HB*) and without heart block (*−HB*). Scale bar, 1mm. **(B)** Heart weight to body weight ratios of *WT* (n = 15), *Trpm7* $^{\alpha MHC/-}$ *+HB* (n= 7) and *Trpm7* $^{\alpha MHC/-}$ *−HB* (n = 10). Fractional shortening **(C)**, left ventricular dimension in diastole (LVID, d) **(D)**, calculated corrected left ventricular mass **(E)**, and heart rate **(F),** on transthoracic echocardiography in 4 week old *WT* controls (*Trpm7*$^{fl/-}$, n = 10; *Trpm7*$^{fl/fl}$, n=9, black bars) compared to litter-mate *Trpm7* $^{\alpha MHC/-}$ mice with HB (*red bar*, n = 4) and without HB (*blue bar*, n = 5) . **(G)** *WT* and **(H)** *Trpm7* $^{\alpha MHC/-}$ *+HB* ventricular cardiomyocytes enzymatically dissociated, fixed (4% PFA) and immunostained for cardiac troponin (*TnI: red*). Nuclei stained with DAPI (*blue*). Scale bar, 100 μm. (**I**) Quantification of cardiomyocyte surface area (n = 46), length (n = 49) and width (n = 52) from *WT* and *Trpm7* $^{\alpha MHC/-}$ *+HB* (n = 49/35/35). * $p < 0.05$, ** $p < 0.01$, *** $p < 0.001$ compared to age matched *WT (Trpm7*$^{fl/fl}$*)* NS; not statistically significant.

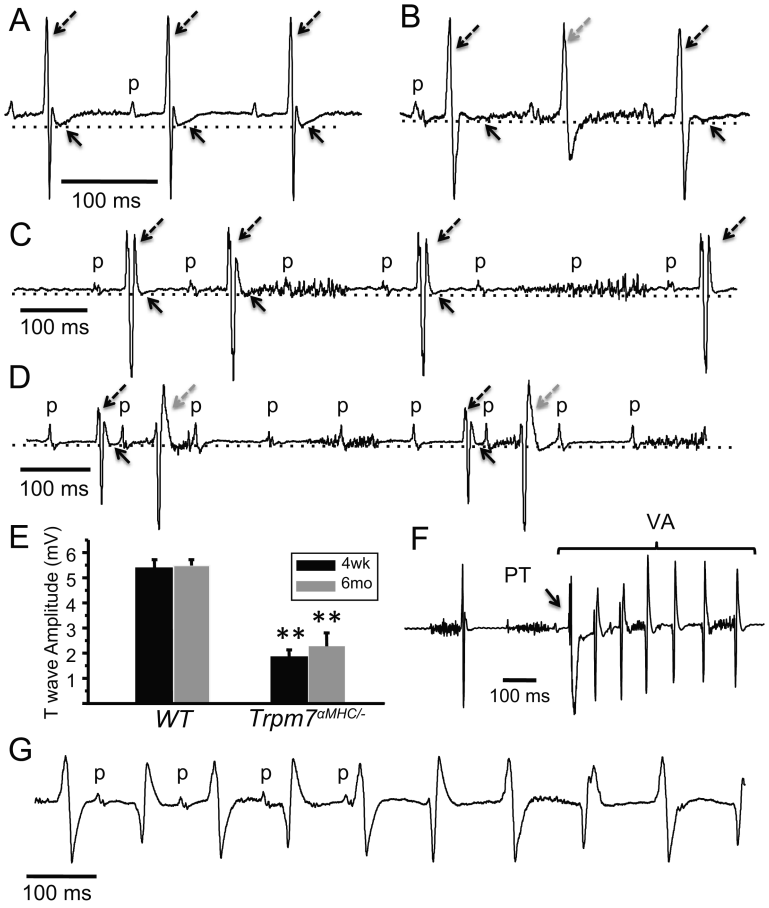

Figure 4.

Trpm7 $^{\alpha MHC/-}$ mice exhibit high-grade atrioventricular block, T wave flattening, and ventricular arrhythmias. **(A)** Normal sinus rhythm (p denote P waves; atrial depolarization) with intact atrioventricular conduction and normal ventricular repolarization (T wave amplitude) (*dotted line, solid arrows*) in the ECG of a sedated *WT* mouse. **(B)** 2:1 **(C)** 3:2/3:1 and **(D)** 5:1 second degree atrioventricular block and reduced T wave amplitude (*dotted line, solid arrows)* in ECGs of sedated *Trpm7* $^{\alpha MHC/-}$ mice: ***broken black arrow*** = conducted beat, ***broken grey arrow*** = ectopic ventricular beat/fusion beat. **(E)** T wave amplitude is depressed in *Trpm7* $^{\alpha MHC/-}$ (n = 8) compared to *WT* (n = 6) mice at both 4 weeks- and 6 months-of-age. **(F)** Ventricular arrhythmia (VA) induced by mechanical stimulation (PT) on a dispersed T wave in a *Trpm7* $^{\alpha MHC/-}$ mouse. **(G)** Sustained bidirectional ventricular arrhythmia (VA) captured in 30% of affected *Trpm7* $^{\alpha MHC/-}$ mice. VA episodes typically lasted 30-100 beats and spontaneously terminate. ** $p < 0.01$.

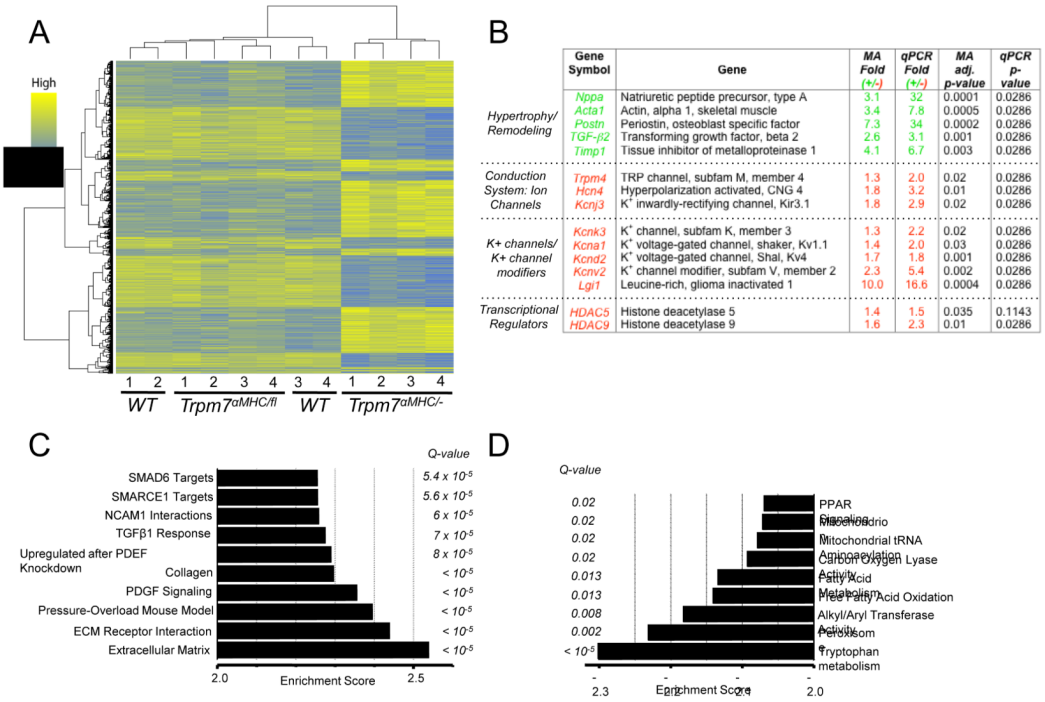

Gene Symbol	Gene	MA Fold (+/-)	qPCR Fold (+/-)	MA adj. p-value	qPCR p-value
Hypertrophy/ Remodeling					
Nppa	Natriuretic peptide precursor, type A	3.1	32	0.0001	0.0286
Acta1	Actin, alpha 1, skeletal muscle	3.4	7.8	0.0005	0.0286
Postn	Periostin, osteoblast specific factor	7.3	34	0.0002	0.0286
TGF-β2	Transforming growth factor, beta 2	2.6	3.1	0.001	0.0286
Timp1	Tissue inhibitor of metalloproteinase 1	4.1	6.7	0.003	0.0286
Conduction System: Ion Channels					
Trpm4	TRP channel, subfam M, member 4	1.3	2.0	0.02	0.0286
Hcn4	Hyperpolarization activated, CNG 4	1.8	3.2	0.01	0.0286
Kcnj3	K^+ inwardly-rectifying channel, Kir3.1	1.8	2.9	0.02	0.0286
K+ channels/ K+ channel modifiers					
Kcnk3	K^+ channel, subfam K, member 3	1.3	2.2	0.02	0.0286
Kcna1	K^+ voltage-gated channel, shaker, Kv1.1	1.4	2.0	0.03	0.0286
Kcnd2	K^+ voltage-gated channel, Shal, Kv4	1.7	1.8	0.001	0.0286
Kcnv2	K^+ channel modifier, subfam V, member 2	2.3	5.4	0.002	0.0286
Lgi1	Leucine-rich, glioma inactivated 1	10.0	16.6	0.0004	0.0286
Transcriptional Regulators					
HDAC5	Histone deacetylase 5	1.4	1.5	0.035	0.1143
HDAC9	Histone deacetylase 9	1.6	2.3	0.01	0.0286

Figure 5.

Myocardial transcriptional profile is altered in *Trpm7* $^{\alpha MHC/-}$ ventricular tissue. **(A)** Heat map displaying 2-way hierarchical clustering and expression levels of differentially expressed genes in *WT*, *Trpm7* $^{\alpha MHC/fl}$ and *Trpm7* $^{\alpha MHC/-}$ hearts (each column 1-4 represents RNA pooled from 2 hearts). ~1300 genes were differentially expressed in *Trpm7* $^{\alpha MHC/-}$ hearts based on an adjusted p-value < 0.05 and a > 1.3-fold change relative to *WT*. **(B)** Selected up-regulated and down-regulated genes from microarray (MA) analysis and validation by qPCR. *Green (+): fold upregulated* and *Red (−): fold down regulated*. **(C-D)**. Gene Set Enrichment Analysis (GSEA) revealing pathways and processes enriched in *Trpm7* $^{\alpha MHC/-}$ compared to *WT* **(C)** and negatively enriched **(D)**. Q-value: False Discovery Rate (FDR) adjusted p-value. Q < 0.05 is statistically significant.

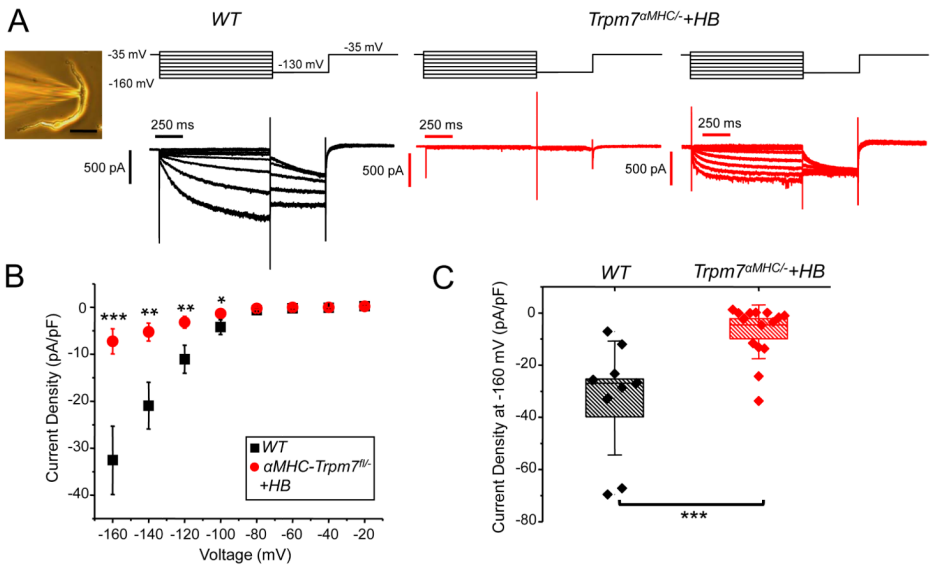

Figure 6.

Trpm7 deletion significantly diminishes I_f in isolated atrioventricular nodal cells. **(A)** *Inset:* patch-clamped atrioventricular nodal cell (AVN): AVN were identified by their characteristic spindle-like morphology and lower cell capacitance, ranging from 20-40 pF ($Cap_{AVN\text{-}WT}$ = 31 ± 2 pF, n= 9; $Cap_{AVN-KO+HB}$ = 36 ± 4, n = 15, p = 0.4). Hyperpolarization-activated current traces, I_f, from *WT* (**black: left**) and *Trpm7* $^{\alpha MHC/-}$ *+HB* (**red: center, right**). Voltage protocols are shown above current traces. I_f was abolished in several AVN cells from *Trpm7* $^{\alpha MHC/-}$ *+HB* (6/15, **center**). In some AVN cells from *Trpm7* $^{\alpha MHC/-}$ *+HB*, I_f had more rapid activation kinetics consistent with I_f contributed by *Hcn2* (**right**). **(B)** I_f current-voltage relationship from AVN of *WT* (■, n = 9) and *Trpm7* $^{\alpha MHC/-}$ *+HB* (●, n = 15). I_f is significantly diminished in *Trpm7* $^{\alpha MHC/-}$ *+HB* AVN compared to *WT* AVN at multiple membrane potentials. Error bars represent standard error of the mean. **(C)** Box plots with overlying data points showing the distribution of I_f current densities at −160 mV from *WT* (black, n = 9) and *Trpm7* $^{\alpha MHC/-}$ *+HB* (red, n = 15) AVN cells. In box plots, error bars represent the standard deviation of the mean. Box height represents the standard error. * $p < 0.05$, ** $p < 0.01$, *** $p < 0.001$.

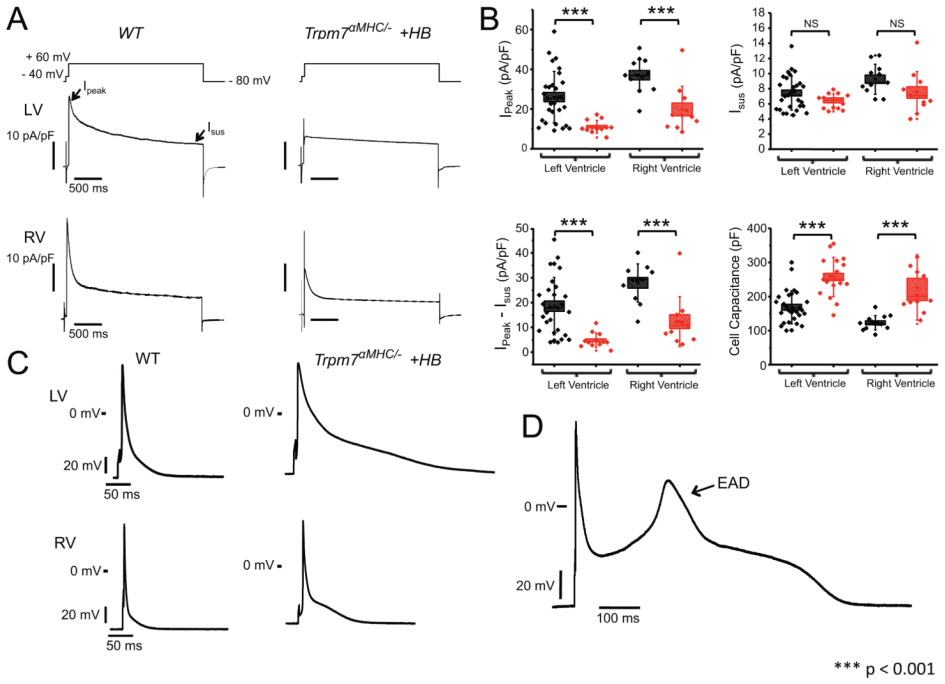

Figure 7.

Transient outward current is diminished and action potentials prolonged in ventricular cells from *Trpm7* $^{\alpha MHC/-}$ mice with heart block. **(A)** Outward potassium current recorded from *WT* (**left**) and *Trpm7* $^{\alpha MHC/-}$ *+HB* (**right**) ventricular myocytes from left ventricle (LV: **top**) and right ventricle (RV: **bottom**) in response to a 2.5 s voltage step to +60 mV after a 50 ms step to −40 mV from a holding potential of −80 mV. Peak outward potassium current (I_{peak}) and sustained outward potassium current (I_{sus}) are indicated (**arrows**). **(B)** Box plots with overlying data points showing the distribution of I_{peak} (**top left**), I_{sus} (**top right**), $I_{peak} - I_{sus}$ (I_{to}, **bottom left**) current densities at +60 mV and cell capacitance (**bottom right**) from *WT* (black, n = 29, LV; n = 11, RV) and α*MHC-Cre-Trpm7*$^{fl/-}$ *+HB* (red, n = 12-17, LV; n = 11, RV)) left and right ventricular myocytes. **(C)** Representative action potentials measured in current-clamp mode from *WT* (**left**) and *Trpm7* $^{\alpha MHC/-}$ *+HB* (**right**) from LV (**top**) and RV (**bottom**). **(D)** Representative action potential with early after-depolarization (EAD) in a *Trpm7* $^{\alpha MHC/-}$ *+HB* myocyte. Error bars on box plots represent the standard deviation of the mean. Box height represents the standard error. *** $p < 0.001$.

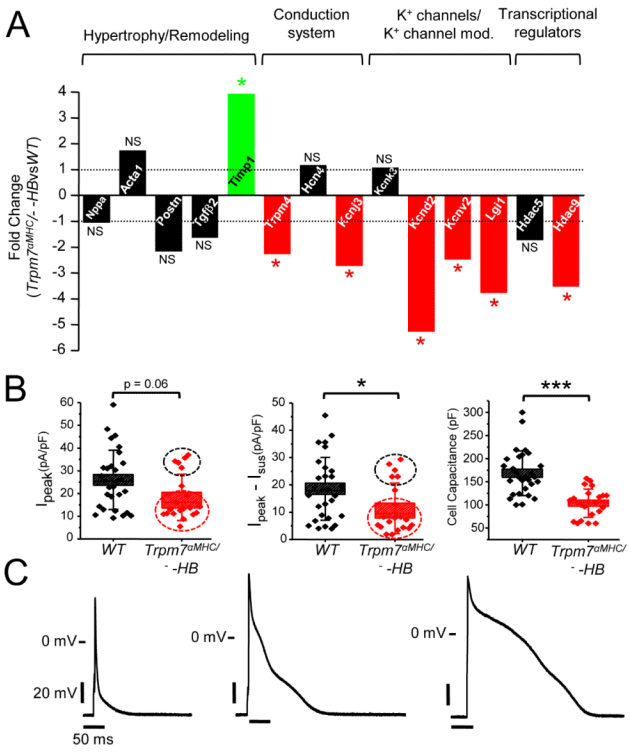

Figure 8.

Kcnd2 expression and I_{to} are diminished and action potentials prolonged in *Trpm7* $^{\alpha MHC/-}$ hearts, independent of cardiac hypertrophy. **(A)** qRT-PCR assessment of mRNA from *Trpm7* $^{\alpha MHC/-}$ *−HB* ventricular tissue (n = 4 hearts) compared to *WT* of the selected gene set examined in *Trpm7* $^{\alpha MHC/-}$ *+HB* hearts. Fold change significantly ($p < 0.05$) increased (green), decreased (red) or unchanged (black). P-values are indicated above or below the bars. **(B)** Box plots with overlying data points showing the distribution of I_{peak} (**left**), $I_{peak} - I_{sus}$ (I_{to}, **center**) current densities at +60 mV and cell capacitance (**right**) from *WT* (black, n = 29) and *Trpm7* $^{\alpha MHC/-}$ *−HB* (red, n = 20-22) left ventricular myocytes. A bimodal distribution of I_{peak} and I_{to} current densities are observed (black and red dashed circles) suggesting a mosaic effect on I_{to} reduction. **(C)** Representative action potentials measured in current-clamp mode from *Trpm7* $^{\alpha MHC/-}$ *−HB* ventricular myocytes, ranging from short *WT*-like (**left**) to moderately (**center**) and severely prolonged (**right**). * $p < 0.05$, *** $p < 0.001$.

Table 1

Action potential (AP) parameters of isolated ventricular myocytes from *WT*, *Trpm7 $^{MHC/fl}$*, *Trpm7 $^{MHC/-}$ +HB and Trpm7 $^{MHC/-}$ −HB* hearts. APDx indicates AP duration to x% repolarization from the peak of the AP. RMP is myocyte resting membrane potential. Peak is the maximum AP membrane potential.

Left Ventricle					
	WT	**Trpm7 $^{MHC/fl}$**	**Trpm7 $^{MHC/-}$ +HB**	**Trpm7 $^{MHC/-}$ −HB**	**n**
APD30 (ms)	2.4±0.3	2.6±0.3	6.5±1.6***	7.1±3.0**	33/24/18/19
APD50 (ms)	5.6±0.8	6.2±0.9	22.2±7.0***	20.0±8.0**	33/24/18/19
APD70 (ms)	10.8±1.4	11.3±1.6	100.3±41.1***	34.4±11**	33/24/18/19
APD90 (ms)	35.8±3.7	43.4±5.1	207.6±50.5***	81.4±13.8***	33/24/18/19
RMP (mV)	−71.6±0.7	*ND*	−70.3±0.6	−74.0±0.7*	33/24/18/19
Peak (mV)	55.3±1.0	*ND*	57.9±0.6	51.7±2.7	33/24/18/19
Right Ventricle					
	WT	***Trpm7$^{\alpha MHC/fl}$***	***Trpm7$^{\alpha MHC/-}$ +HB***	***Trpm7$^{\alpha MHC/-}$ −HB***	***n***
APD30 (ms)	1.4±0.1	*ND*	3.0±0.5**	*ND*	13/13
APD50 (ms)	2.7±0.3	*ND*	7.0±1.4**	*ND*	13/13
APD70 (ms)	5.6±0.8	*ND*	14.8±3.0**	*ND*	13/13
APD90 (ms)	16.9±2.4	*ND*	71.8±15.6**	*ND*	13/13
RMP (mV)	−71.9±0.9	*ND*	−72.8±0.3	*ND*	13/13
Peak (mV)	55.6±1.4	*ND*	56.1±0.8	*ND*	13/13

* P<0.05;

** P<0.01;

*** P<0.001; compared to *WT*. *ND*, not determined. n, indicates number of myocytes in each group in order of columns from left to right.